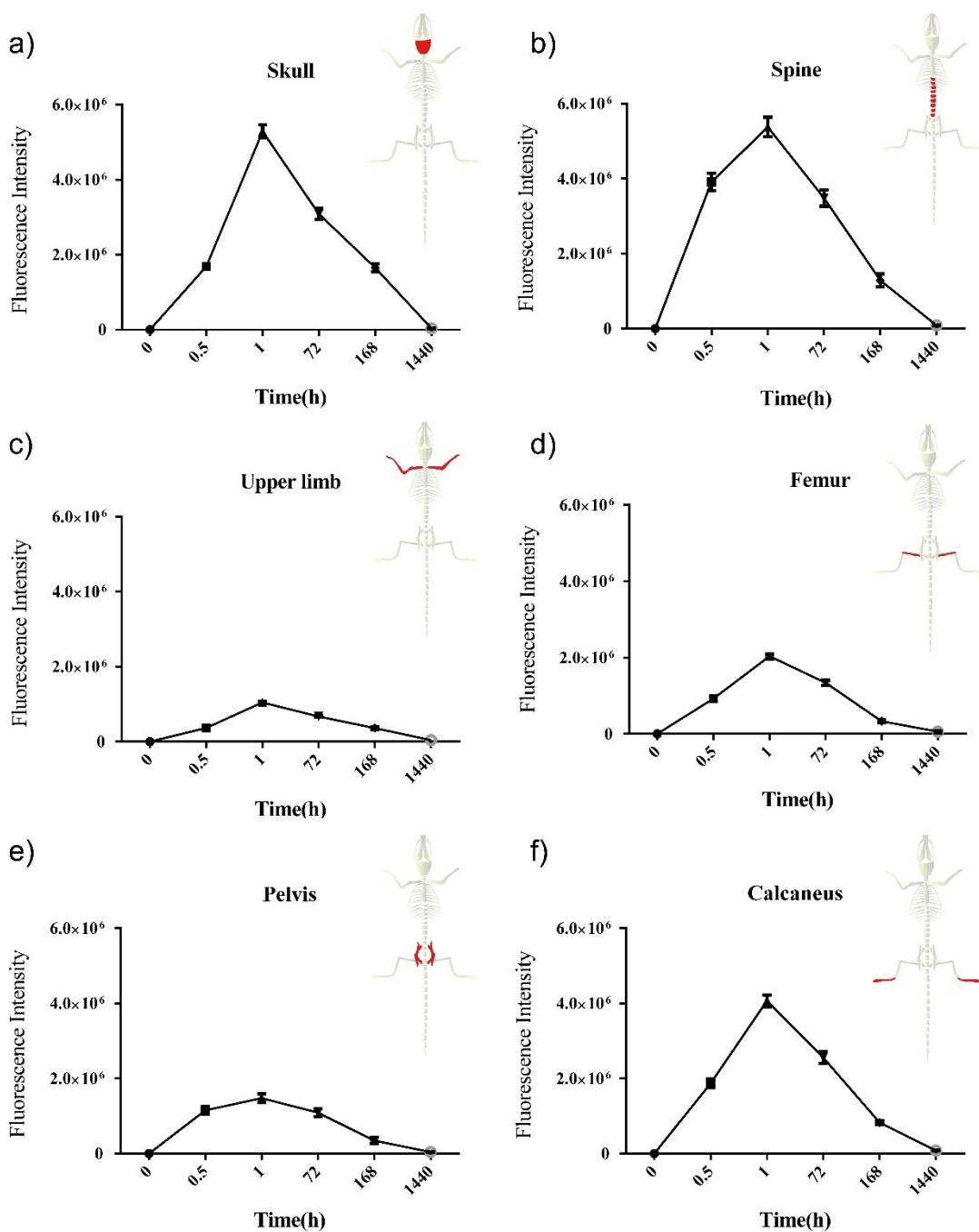


Supporting Information

In vivo Live Imaging of Bone Using Shortwave Infrared Fluorescence Quantum Dots

Yanjun Che^{1,2,#}, Sijia Feng^{3,#}, Jiangbo Guo^{1,#}, Junjun Hou⁴, Xuesong Zhu¹, Liang Chen¹, Huilin Yang¹, Mo Chen³, Yunxia Li³, Shiyi Chen³, Zhen Cheng^{5,*}, Zongping Luo^{1,*}, Jun Chen^{3,*}



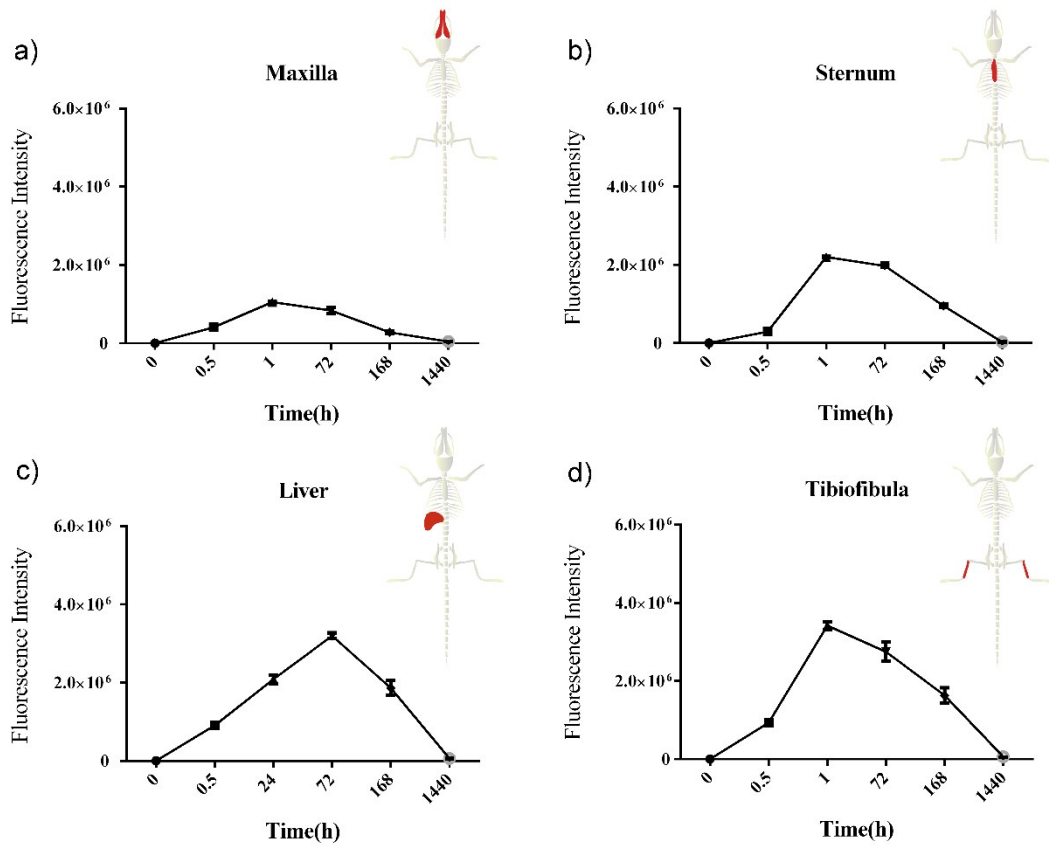


Figure S1. (a-d) Real-time fluorescence Intensity analysis of Balb/C nude mouse by RNase A-PbS QDs (anterior view).

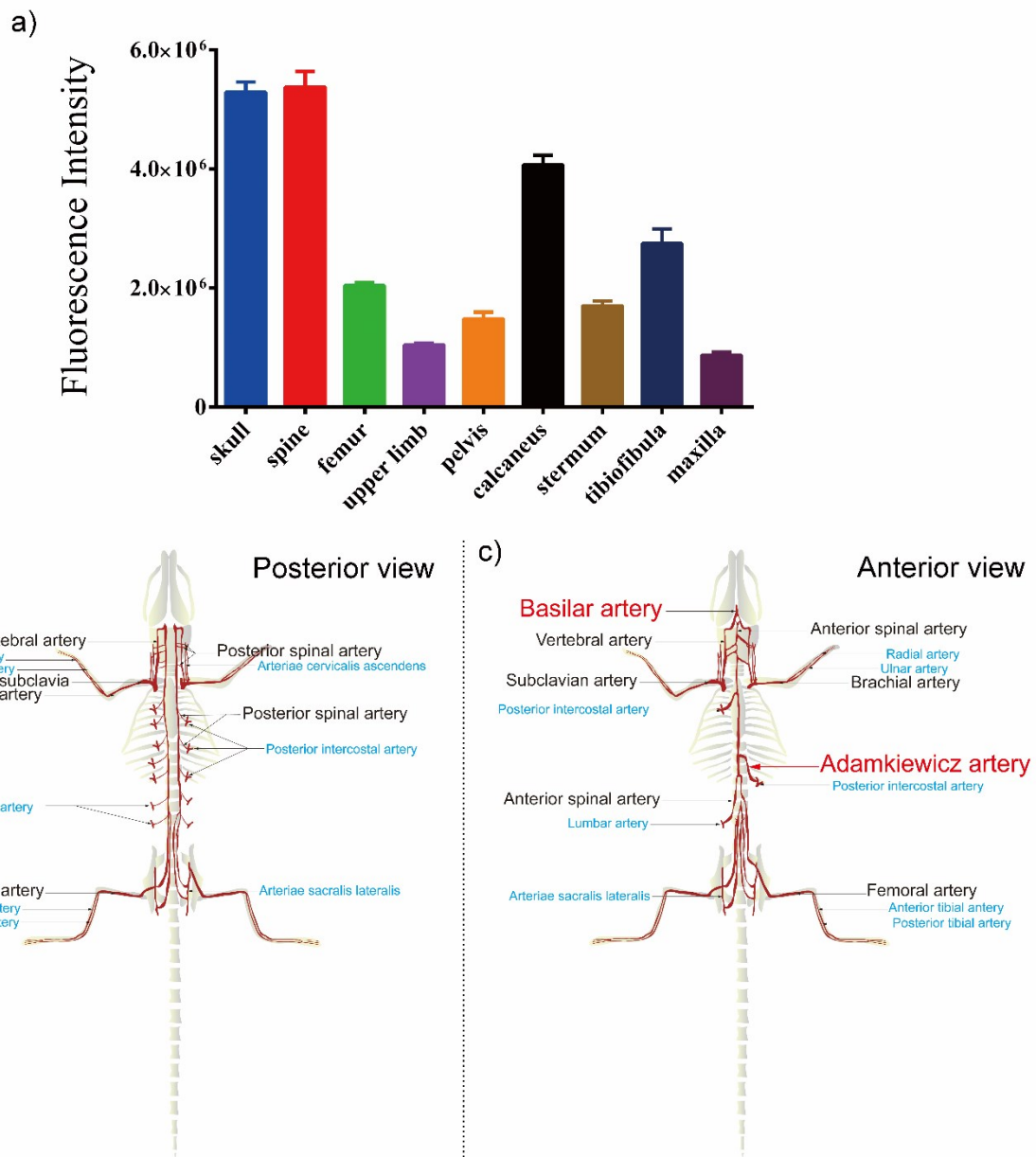


Figure S2. (a) The fluorescence intensity of various bone structures at 1 h post-injection. Schematic diagram of spinal blood supply from (b) posterior view and (c) anterior view (red arrow: the Adamkiewicz artery)

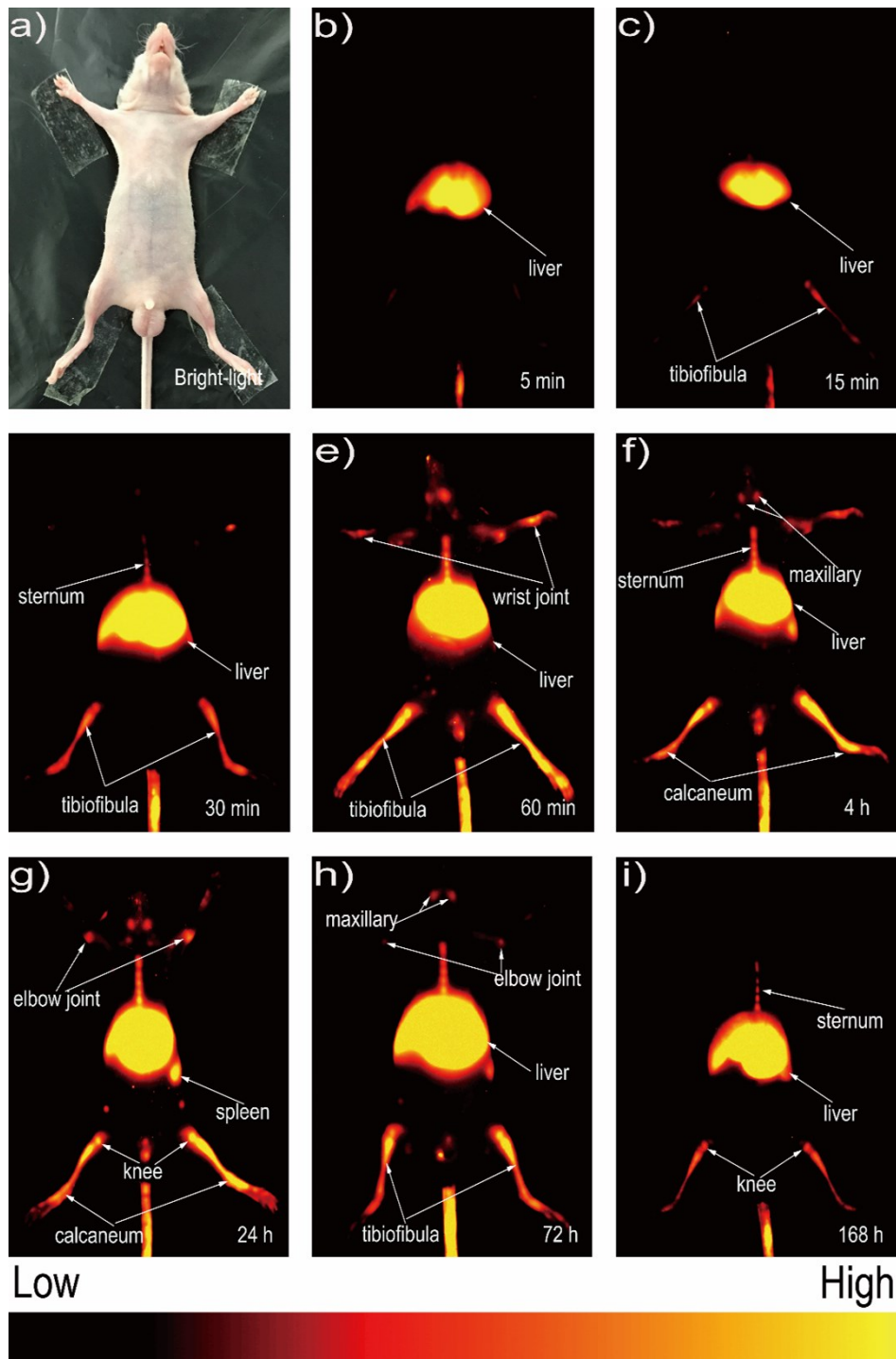


Figure S3. (a) Photo of Balb/C nude mouse. (b-i) Real-time fluorescence imaging of Balb/C nude mouse by RNase A-PbS QDs (anterior view).

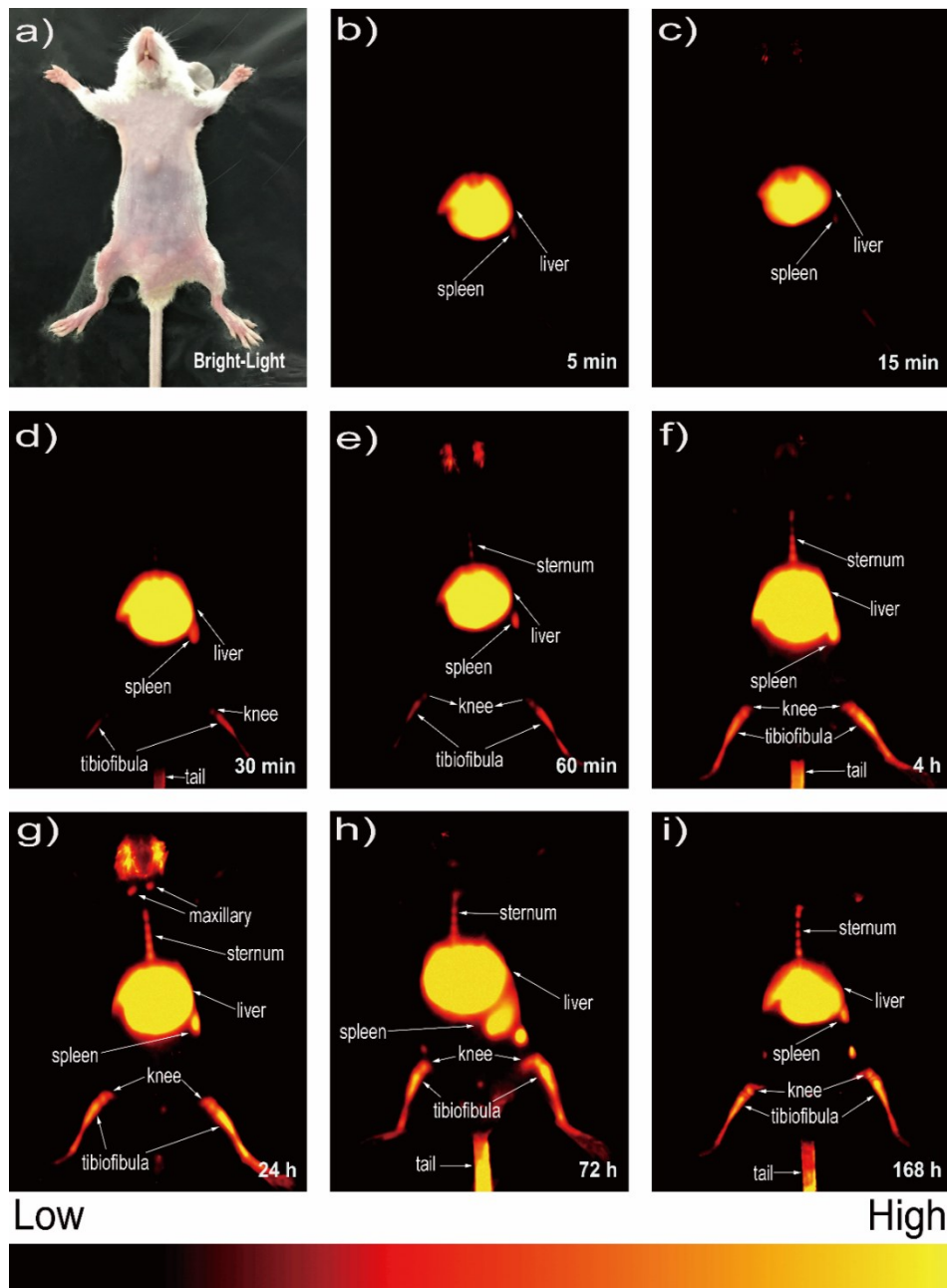


Figure S4. (a) Photo of Balb/C mouse. (b-i) Real-time SWIR fluorescence imaging of Balb/C mouse by RNase A-PbS QDs (anterior view) with images acquired at 5 min, 15 min, 30 min, 60 min, 4 h, 24 h, 72 h and 168 h post-injection, respectively.

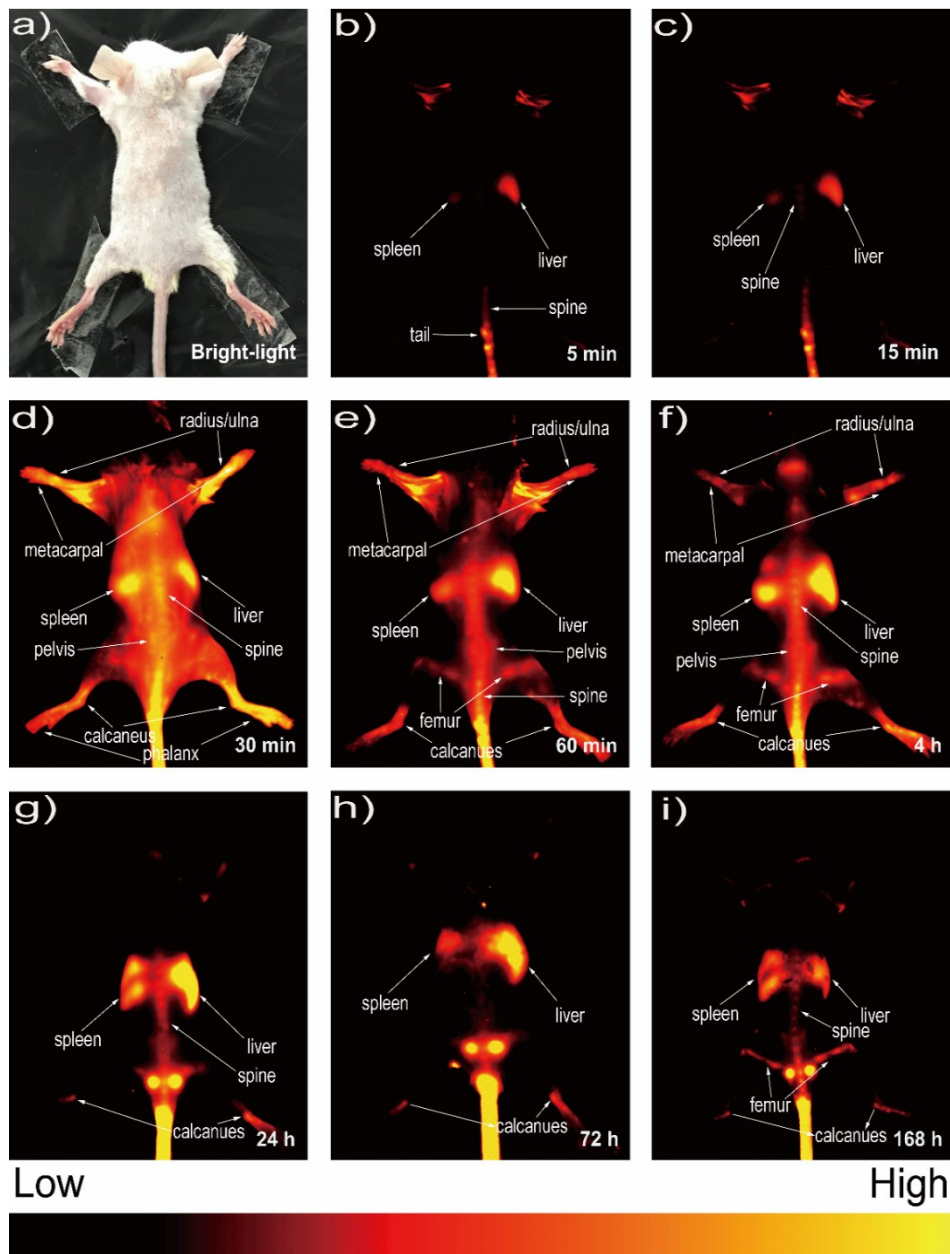


Figure S5. (a) Photo of Balb/C mouse. (b-i) Real-time SWIR fluorescence imaging of Balb/C mouse by RNase A-PbS QDs (posterior view) with images acquired at 5 min, 15 min, 30 min, 60 min, 4 h, 24 h, 72 h and 168 h post-injection, respectively.

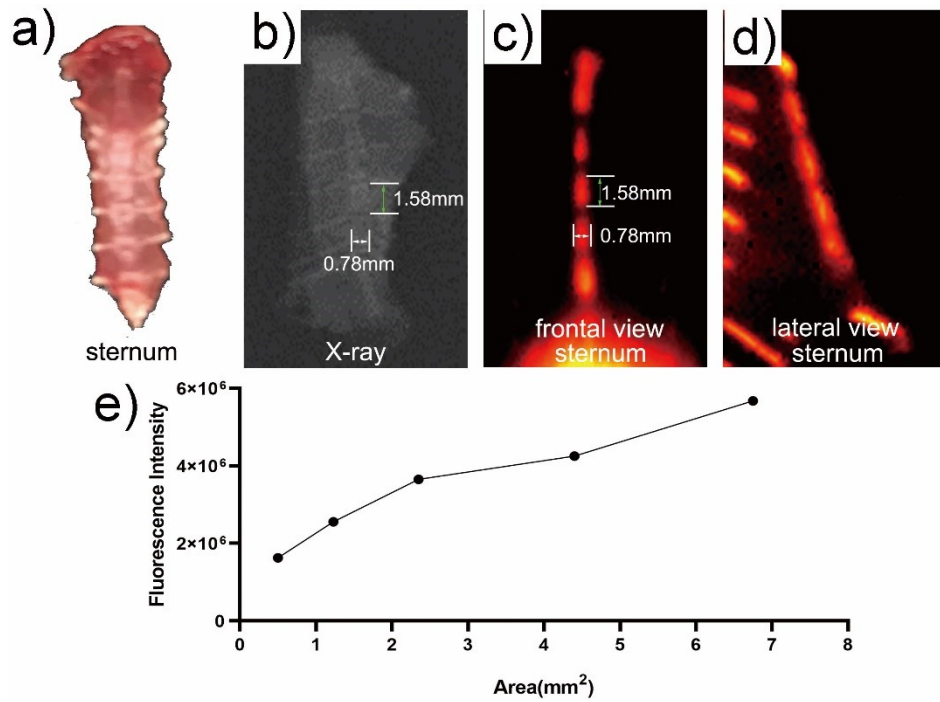


Figure S6. (i) Specimen model of the sternum. (j) X-ray photo of the sternum. (k) SWIR image of the sternum from frontal view (posteroanterior position). (l) SWIR image of the sternum from lateral view (lateral position). The inserted pictures in (b) and (d-h) were corresponding X-ray photos. (m) Corresponding fluorescence intensity analysis.

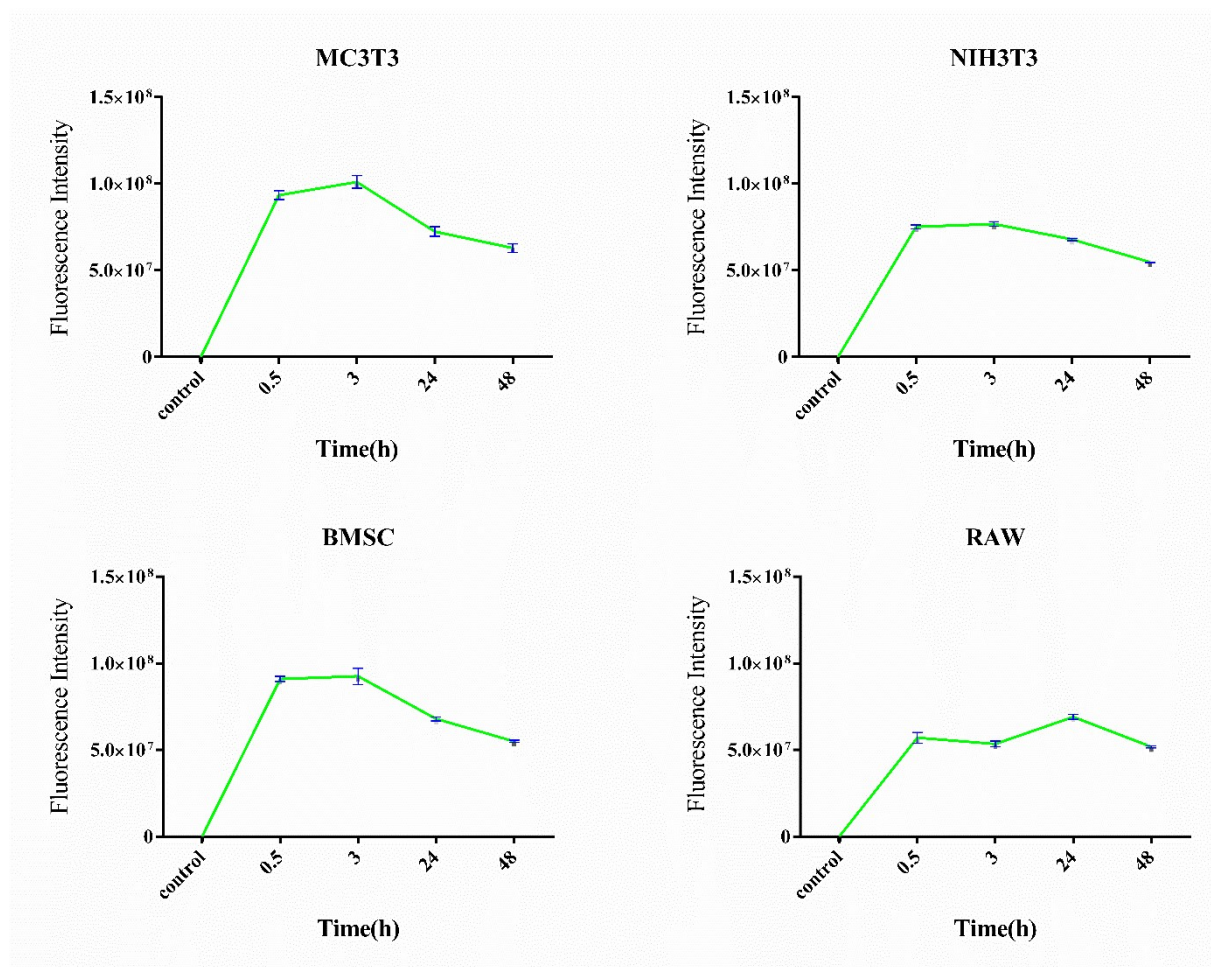


Figure S7. (a-d) Statistical analysis of the imaging of four cell types by RNase A-PbS QDs before PBS rinsing.

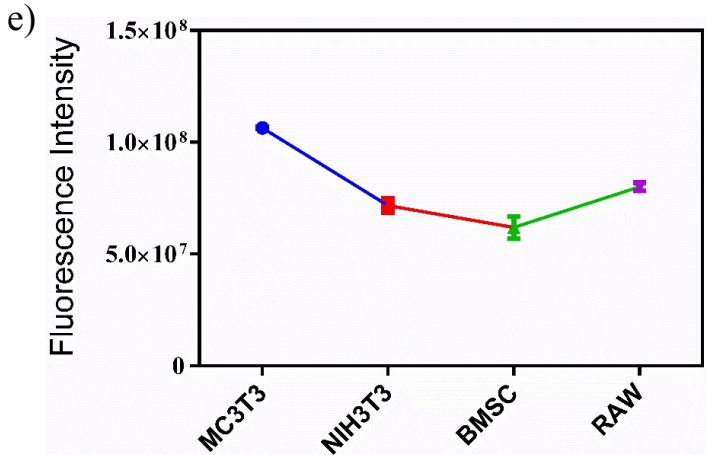
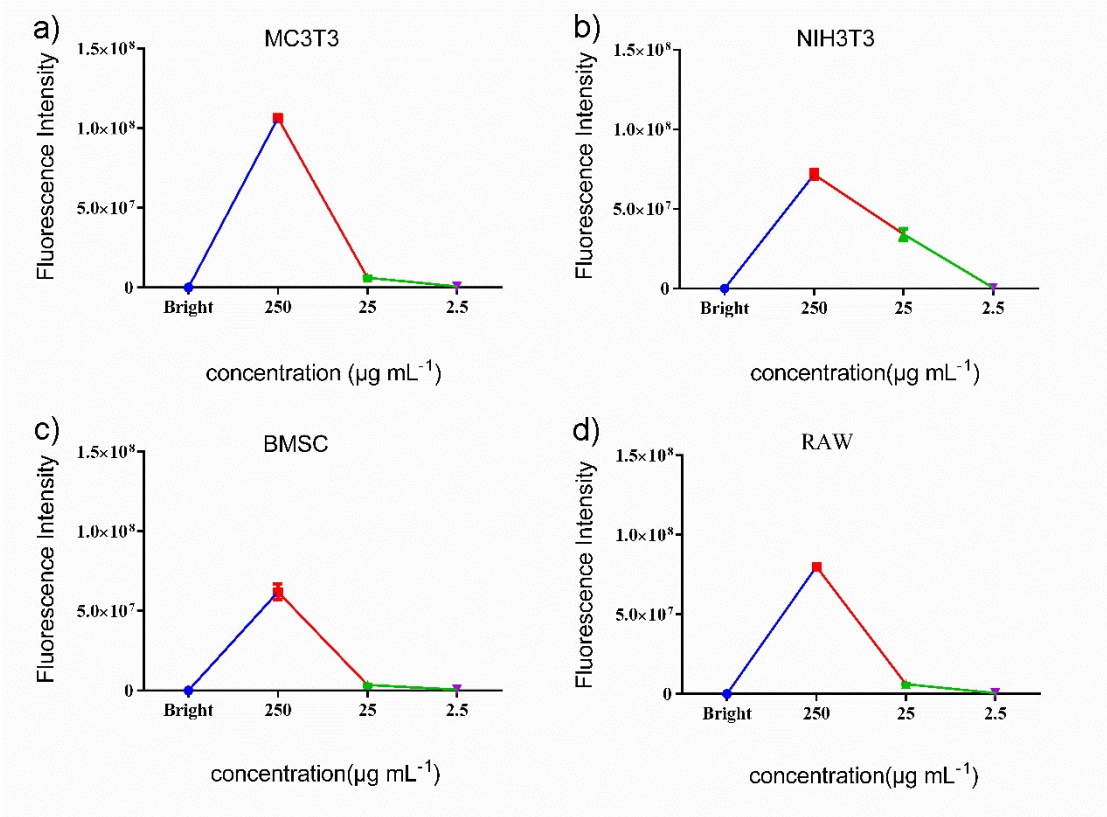


Figure S8. (a-d) Statistical analysis of the variation of QDs fluorescence intensity regarding the concentration of QDs solution. (e) FL intensity of four cell types incubated with QDs at the same concentration of 250 $\mu\text{g mL}^{-1}$.

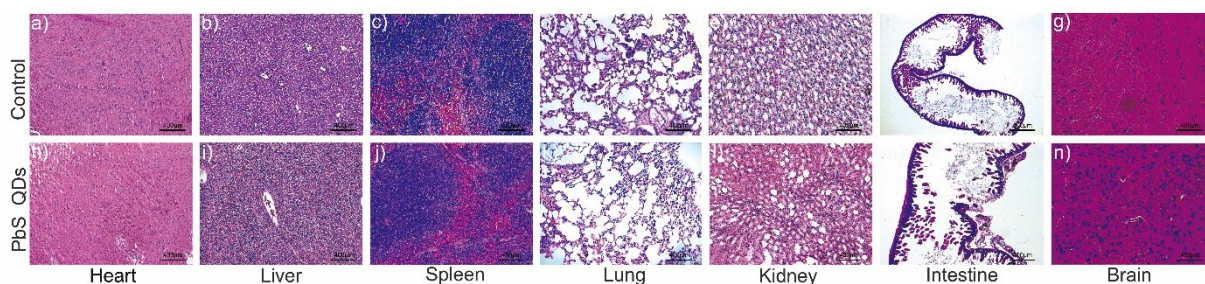


Figure S9. (a-n) Histological analysis of major organs before and after QDs injection (scale bar: 400 μ m).

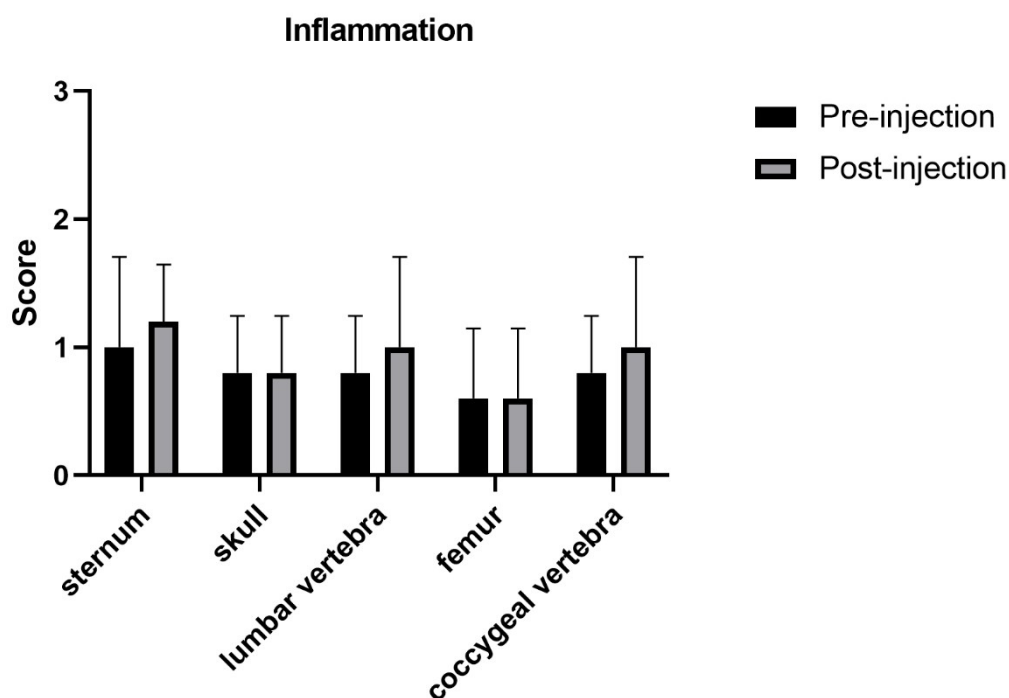


Figure S10. Pathological score of histological analysis of major bones before and after QDs injection

Experimental Section

Synthesis and surface modification of SWIR RNase A-PbS QDs: SWIR RNase A-PbS QDs was prepared according to previous studies¹⁻³. In brief, 500 μ l RNase A (50 mg/ml) was mixed with 500 μ l Pb(CH₃COO)₂ (10 mM). Then, the mixed solution was stirred for 5 min at room temperature with the pH adjusted to 7.5 using 1 M NaOH. After that, 300 μ l Na₂S (10 mM) was added to the mixture, which was then heated in a microwave reactor for 30 s at 100 $^{\circ}$ C. Finally, the as-prepared RNase A-PbS QDs solution was stored at 4 $^{\circ}$ C in darkness.

Characterization of the RNase A-PbS QDs: Transmission electron microscopy (TEM) and high-resolution TEM (HRTEM) images were recorded from a JEOLJEM-2010F electron microscope with an accelerating voltage of 200 kV. Photoluminescence (PL) spectra were obtained from a Shimadzu RF-6310PC spectrofluorometer with 685 nm excitation. The RNase A-PbS QDs showed a stable photoluminescence for 2 hours with 808 nm excitation (123.8 mW/cm²).

Experimental Animals: 5 male Balb/C nude mice (4 weeks) and 5 male Balb/C mice (6 weeks) were kept under the same standard circumstances. This study was performed in strict accordance with the NIH guidelines for the care and use of laboratory animals (NIH Publication No. 85-23 Rev. 1985) and was approved by the Institutional Animal Care Committee of the Laboratory Animal at the School of Medicine, Soochow University (Suzhou, China). Informed consent was obtained for any experimentation with animal subjects.

In vivo Imaging Study: After the mice were anesthetized with isoflurane inhalation, 200 μ L of RNase A-PbS QDs (\sim 26 nM, dosage: \sim 1 μ g per mouse) was injected through tail vein. Right after the injection, fluorescence signals were recorded at different time points over 1440 hours (2 months). At each time point, the mice were sacrificed to harvest the major organs and bone tissues for *ex vivo* imaging and H.E staining. An 808 nm diode laser with both 850 nm and 1000 nm short-pass filters was used as excitation source (power density: 15 mW/cm², exposure time: 100 ms). In order to achieve NIR-II fluorescence images with an InGaAs CCD camera, emission signals were filtered by a 1100 nm long-pass filter.

Ex vivo Imaging Study: The Human BM-MSCs, murine macrophage-like cells (RAW264.7), mouse osteoblastic cells (MC3T3-E1) and mouse embryonic fibroblast cells (NIH3T3) were

incubated overnight with RNase A-PbS QDs diluted by the original medium respectively (DMEM for RAW264.7, α -MEM for BM-MSCs, MC3T3-E1 and NIH3T3) at 5X, 10X and 50X. Then the cells were observed under infrared microscope. After that, RNase A-PbS QDs was removed from the cells of 5X. The remaining cells were rinsed by PBS (Procell Life Science & Technology Co Ltd, Wu Han, China) twice and again cultured with respective medium. Observation under infrared microscope was done at 0.5 h, 3 h, 24 h, 48 h and 72 h post-rinsing. No fluorescence was observed at 72 h post-rinsing due to cell death. On the other hand, the cells of 10X and 50X (not rinsed by PBS) were under constant culture and observed in the same time course.

Cell Culture: Human BM-MSCs (Cyagen Biosciences Inc., Guangzhou, China) were cultured in α -MEM (Thermo Fisher Scientific, Waltham, MA, USA) supplemented with 10% fetal bovine serum (FBS, Thermo Fisher Scientific), 100 U/mL of penicillin, and 100 μ g/mL of streptomycin (Thermo Fisher Scientific) in a humidified 37°C/5% CO₂ incubator with medium changed every three days. Murine macrophage-like cells (RAW264.7), purchased from the CBCAS (Cell Bank of the Chinese Academy of Sciences, Shanghai, PR China), were cultured in DMEM/HIGH GLUCOSE (HyClone, Logan, Utah, USA) supplemented with 10% FBS (Thermo Fisher Scientific), 100 U/mL of penicillin, and 100 μ g/mL of streptomycin (Thermo Fisher Scientific) in a humidified 37°C/5% CO₂ incubator with medium change every three days. The mouse osteoblastic cells (MC3T3-E1) and mouse embryonic fibroblast cells (NIH3T3), purchased from the CBCAS, were cultured in α -MEM (Thermo Fisher Scientific) supplemented with 10% FBS (Thermo Fisher Scientific), 100 U/mL of penicillin, and 100 μ g/mL of streptomycin (Thermo Fisher Scientific) in a humidified 37°C/5% CO₂ incubator with medium changed every three days.

Histological Analysis: Bone tissue samples were fixed in 10% neutral formalin solution (Shanghai Yuanye Bio-Technology Co Ltd, Shanghai, China) for 24 hours, and decalcified with 10% ethylenediaminetetraacetic acid (Biosharp, Hefei, China) for 30 days. The samples were then paraffin-embedded (Leica, Richmond, USA) for serial sectioning using a histotome (Leica, Heidelberg, Germany) to a thickness of 6 μm . Organ tissue samples did not have decalcification steps, the rest were the same as for bone tissue samples. Hematoxylin-eosin staining were carried out on the bone tissue and organ tissue sections according to the kit instructions (Beijing Solarbio Science & Technology Co Ltd, Beijing, China). Briefly, hematoxylin stained for 5 min and eosin stained for 1 min. The stained images were visualized using a binocular microscope (XSP-2CA, Shanghai, China). The pathological score was calculated according to previous literature.⁴

References

1. J. Chen, Y. Kong, W. Wang, H. Fang, Y. Wo, D. Zhou, Z. Wu, Y. Li and S. Chen, *Chem Commun (Camb)*, 2016, **52**, 4025-4028.
2. Y. Kong, J. Chen, H. Fang, G. Heath, Y. Wo, W. Wang, Y. Li, Y. Guo, S. D. Evans, S. Chen and D. Zhou, *Chem Mater*, 2016, **28**, 3041-3050.
3. S. Feng, J. Chen, Y. Wo, Y. Li, S. Chen, Y. Zhang and W. Zhang, *Biomaterials*, 2016, **103**, 256-264.
4. D. S. Suh, J. K. Lee, J. C. Yoo, S. H. Woo, G. R. Kim, J. W. Kim, N. Y. Choi, Y. Kim and H. S. Song, *Am J Sports Med*, 2017, **45**, 2019-2027.